





Article

Tailoring Epoxy Composites with *Acacia caesia* Bark Fibers: Evaluating the Effects of Fiber Amount and Length on Material Characteristics

Sivasubramanian Palanisamy ^{1,2,*} , Mayandi Kalimuthu ² , Carlo Santulli ³ , Murugesan Palaniappan ⁴, Rajini Nagarajan ⁴ and Cristiano Fragassa ^{5,*} 

¹ Department of Mechanical Engineering, Dilkap Research Institute of Engineering and Management Studies, Neral, Raigad 410101, Maharashtra, India

² Department of Mechanical Engineering, Kalasalingam Academy of Research and Education, Anand Nagar, Krishnankovil, Srivilliputhur 626126, Tamilnadu, India; k.mayandi@gmail.com

³ School of Science and Technology, Università degli Studi di Camerino, 62032 Camerino, Italy; carlo.santulli@unicam.it

⁴ Department of Mechanical Engineering, College of Engineering, Imam Mohammed Ibn Saud Islamic University, Riyadh 11432, Saudi Arabia; mpapathi@imamu.edu.sa (M.P.); n.rajini@klu.ac.in (R.N.)

⁵ Department of Industrial Engineering, Alma Mater Studiorum, University of Bologna, 40136 Bologna, Italy

* Correspondence: sivaresh948@gmail.com (S.P.); cristiano.fragassa@unibo.it (C.F.)

Abstract: In recent years, there has been growing interest in utilizing bark fibers as reinforcements for polymer composites. This study focused on the characterization of epoxy composites reinforced with *Acacia caesia* bark (ACB) fibers, considering their mechanical, morphological, and thermal properties. Various amounts of ACB fibers with three different lengths (10, 20, and 30 mm) were incorporated into the composites, ranging from 10 to 35 wt.% in 5% increments. This resulted in 18 sample categories, which were compared to neat epoxy samples. The findings demonstrated that the introduction of ACB fibers, even at the highest fiber content, led to improved mechanical performance. However, a transition in fiber length from 20 to 30 mm exhibited conflicting effects on the composite, likely due to the tendency of bark fibers to bend and split into fibrils during loading. Regarding thermal degradation, the advantages over neat epoxy were evident, particularly for 20 mm fibers, suggesting enhanced interfacial bonding between the matrix and the reinforcement. The epoxy adequately protected the bark fibers, enabling the composite to withstand degradation at temperatures comparable to pure resin, with minimal structural damage below 320 °C.

Keywords: epoxy composites; bark fibers; mechanical properties; Shore D hardness; Izod impact; thermal properties; fracture morphology



Citation: Palanisamy, S.; Kalimuthu, M.; Santulli, C.; Palaniappan, M.; Nagarajan, R.; Fragassa, C. Tailoring Epoxy Composites with *Acacia caesia* Bark Fibers: Evaluating the Effects of Fiber Amount and Length on Material Characteristics. *Fibers* **2023**, *11*, 63. <https://doi.org/10.3390/fib11070063>

Academic Editor: Faiz Shaikh

Received: 3 June 2023

Revised: 11 July 2023

Accepted: 13 July 2023

Published: 17 July 2023



Copyright: © 2023 by the authors. Licensee MDPI, Basel, Switzerland. This article is an open access article distributed under the terms and conditions of the Creative Commons Attribution (CC BY) license (<https://creativecommons.org/licenses/by/4.0/>).

1. Introduction

Bark, the external layer of many plants that is relatively rich in lignin, has some uses related to the extraction of phenols [1–3] and other medical, nutraceutical, and cosmetic substances [4–6]. In other cases, if sufficiently porous, is disposed of in the production of active carbons [7,8]. However, in most cases, bark is still considered a by-product and is normally discarded. As the consequence, in recent years, bark fibers from various species have been employed frequently to reinforce polymer matrices. In particular, epoxy matrices are frequently used in bark fiber composites because of the limited variability in the properties of the cured resin, which facilitates the assessment of the contribution of bark fibers to the composite's performance [9].

A number of examples of epoxy resin–bark fiber composites have been developed and characterized over the past years. These studies, though not very numerous, have established some significant points regarding bark fiber/epoxy composites. Among others, a recent study on *Muntingia calabura* bark fiber composites revealed the importance of alkali

treatment, which dissolved some of the non-cellulose components, increasing crystallinity and hence the tensile strength of the composite. However, the interlock bonding between the fiber and the matrix obtained by alkali treatment also resulted in a rougher surface of the fibers and thus a more pronounced brittle behavior [10]. Conversely, treated fibers can be inserted in larger amounts, resulting in an increase in the tensile strength of the composite; a study on *Holoptelea integrifolia* reported the highest performance with 40 wt.% fibers [11]. Lower levels of reinforcement were successfully attempted for other bark fibers, namely 25 wt.% using *Prosopis juliflora* [12], which produced interesting tribological properties [13], and 20 wt.% with *Ziziphus nummularia* [14]; in both cases, considerable concentrations of alkali treatment were used.

All of this is strictly in line with the general trend of making composite materials more eco-sustainable through the use of natural fibers [15–17] as reinforcements or resins with a reduced environmental impact because of their natural compounds [18,19]. Concerning the use of natural fibers in composites, it is worth considering that the tensile strength of lignocellulosic fibers does not show any specific trend related to their length, as indicated in [20]. However, it is likely that the larger interfacial area encountered when reinforcing a polymer matrix with higher amounts of longer stretches of natural fibers would, in principle, improve the mechanical performance of the composite, though the effect is not linear, and therefore, above a certain level of loading, the performance might decrease [21]. In other words, it is possible to elicit an optimal composition and fiber length. This has been confirmed for fibers from a number of vegetable species; for example, it was recently observed in *Cymbopogon flexuosus*, in which it was also revealed that, above a certain weight of fibers, the non-uniform surface of the fibers and their proneness to fibrillation during loading also results in a progressive loss of interface strength [22].

In particular, *Acacia caesia* (AC) bark fiber, also referred to as “soap bark” because of its scrubbing potential, is derived from a perennial leguminous shrub, which is considerably exploited for medical purposes due to its high content of steroids, anthraquinone, glycosides, and flavonoids [23]. AC extract has been also used as a catalyst for the green synthesis of zinc oxide (ZnO) nanoparticles, which have antimicrobial and photocatalytic applications [24]. The first attempts to turn waste by-products from AC into materials referred to the extraction of cellulose nanowhiskers from AC [25]. Further studies on this fiber have been carried out more recently, and the present study aimed to integrate them. In particular, the extraction of ACB fibers and the effect of alkali treatment on their mechanical strength has been investigated; the measurement of a high level of crystallinity, even in the untreated fibers, suggested that their application in composites was possible even at lengths of up to 150 mm [26]. However, tensile testing on AC fibers, keeping their gauge length at 50 mm, offered an indication of the large variability in strength in addition to a notable tendency to wind up during loading, so it was considered prudent to limit work with composites to the application of lower fiber lengths [27].

In this work, the potential application of *Acacia caesia* bark fibers up to 35 wt.% with a length of up to 30 mm to serve as reinforcement in epoxy composites was studied. Unfortunately, to the knowledge of the authors, there are no previous relevant studies on the effect of ACB fiber characteristics (such as type, dimensions, thickness, orientation, ratio, etc.) on the material mechanical properties, whereas there are studies on many other better-investigated fibers and naturally reinforced materials, e.g., [28–31]. By analogy, it can be expected that the length and ratio of ACB fibers could also have a significant impact on the material characteristics, especially considering the following:

- **Mechanical Properties:** Longer fibers tend to enhance the material’s strength, stiffness, and toughness. They provide a continuous load-bearing pathway, which improves the material’s ability to withstand applied forces. Higher fiber ratios, i.e., a higher volume fraction of fibers in the composite, also contribute to increased mechanical properties.
- **Tensile Strength:** Longer fibers generally result in higher tensile strength. As the fiber length increases, the load transfer between the fibers becomes more efficient, leading

to improved strength characteristics. Shorter fibers may have weaker bonding with the matrix, limiting the overall tensile strength.

- **Flexural Strength:** Longer fibers can enhance the flexural strength of the composite. They provide resistance against bending forces and help distribute the load more effectively. A higher fiber ratio also improves flexural strength.
- **Impact Resistance:** Longer fibers contribute to better impact resistance in composites. They help absorb and distribute the impact energy, preventing crack propagation and increasing the material's ability to withstand sudden loads. Higher fiber ratios further enhance impact resistance.
- **Interfacial Bonding:** The length and ratio of fibers influence the bonding between the fibers and the matrix material. Longer fibers provide a larger surface area for bonding, resulting in improved interfacial adhesion. A strong interfacial bond is crucial for transferring stresses between the fibers and the matrix, thus enhancing the material's overall strength.
- **Durability:** The fiber length and ratio can impact the durability and fatigue resistance of the composite material. Longer fibers with better interfacial bonding can withstand cyclic loading and repetitive stresses more effectively, thereby improving the material's durability.

It is important to note that achieving an optimal fiber length and ratio depends on the specific application and the type of natural fibers used. Different natural fibers have varying mechanical properties, so the ideal fiber characteristics may vary accordingly. Additionally, processing techniques (including fiber pre-treatments [23,28]), fiber alignment, and composite manufacturing methods) also play a role in determining the final material properties. However, it is also important to consider that, in the case of natural fibers, the presence of defects and the fibrillation phenomena of the fiber tend to increase significantly with length, making the behavior of natural composites much different from what was expected. This makes the need to carry out experimental verifications even more significant.

In this case, the ACB fibers were purposely used as extracted, without any treatment, to clarify whether their geometrical regularity was sufficient for the purpose, considering that chemical modification involves some environmental impact that might reduce the significance of using a waste product as a composite reinforcement.

To elucidate the potential of this composite, tensile strength, flexural strength, Izod impact, and Shore D hardness tests were carried out for all categories of samples, while for selected ones, morphological observations of fracture after tensile, impact tests, and thermal characterization were performed.

2. Materials and Methods

2.1. Fibers' Extraction

Fibers from the *Acacia caesia* (AC) climber plant were collected from the Malayattoor forest in the Ernakulam district, Kerala, India. AC bark fibers (ACBF) were extracted as per the typical operation used for the scrubber application, using a knife, mallet, and wire brush, and in the most difficult cases, completing the operation by hand. The bark stretches were then wetted in water for 15 to 20 days to promote microbial breakdown and subsequently separated by stripping. The diameters of the fibers obtained were variable in the range of 100–150 μm , with an average of 127 μm , as reported in [27], where more information is also available.

2.2. Composites Production

2.2.1. Preparation of Matrix

The epoxy and hardener (trade grade) Araldite LY556 and HY951 (Pidilite Industries Ltd. in Dahej, Bharuch, Gujarat, India), respectively, were prepared at a ratio of 10:1. The weights of the resin and hardener were measured using a two decimal figure weighing machine. In a bowl, the hardeners were blended with epoxy resin using a glass pole to stir well, avoiding air bubbles and, consequently, the formation of pores in the mixture.

Mixing and post-curing reduced the diffusion of air bubbles, though it was not sufficient to ensure their complete disappearance. It might be suggested that the remaining presence of bubbles requires an improvement in the mixing procedure or may require the application of a more suitable resin.

2.2.2. Mold Preparation

A hardened rectangular mild steel plate was prepared with dimensions of 300 mm × 300 mm × 3 mm. The three parts of the mold were the upper portion, the rectangular side plate, and the lower base plate. Before the fabrication of the composite, wax was applied to the mold to ease composite removal. A Compression Molding Machine (CMM) was used to compress the mold after filling it with the matrix–fiber mix or the pure matrix, depending on the variant produced. The pressure and curing time were set, as indicated below, to obtain a minimal loss of material from the mold.

2.2.3. Fabrication of Composites

According to the proportions, the ACB fiber and matrix were weighed separately. Before initiating the fabricating process, the upper and the lower mold die surface were cleaned and waxed. ACB fiber was mixed randomly and kept in the lower mold surface, and then the blend was poured into the mold. A hydraulic pressure of 0.1 bar was applied for 2 min using compression molding. The process was carried out under atmospheric air conditions. Subsequently, the temperature was gradually increased to 80 °C for post-curing. The mold was kept under pressure and temperature for half an hour. The mold plates (bottom and top) were opened after the assessed time and allowed to cool at room temperature. The sample composite plates were subsequently removed from the mold. The aspect of the composite's surface is represented in Figure 1.

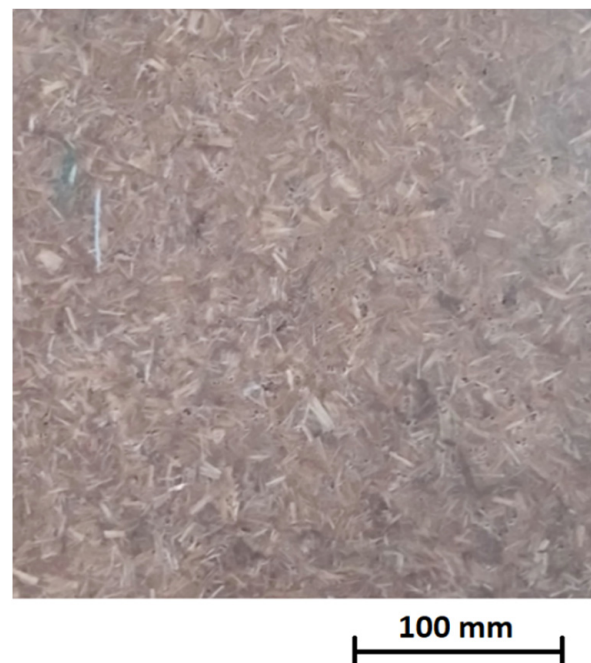


Figure 1. Surface of a composite plate.

The effective combination and impact of the resin/fiber percentage were identified on the basis of different concentrations, such as 90:10, 85:15, 80:20, 75:25, 70:30, and 65:35. Fiber length is one of the critical issues in composites; it also provides an impact and changes in fiber dimensions, namely 10, 20, and 30 mm. Different combinations of composites were manufactured, and the abovementioned proportions were used to manufacture short-fiber composites. The different categories of samples produced are reported in Table 1.

Table 1. Sample categories produced for the study.

Sample No.	Fiber Amount (%)	Fiber Length (mm)
C0	-	-
C1	10	10
C2	15	
C3	20	
C4	25	
C5	30	
C6	35	
C7	10	20
C8	15	
C9	20	
C10	25	
C11	30	
C12	35	
C13	10	30
C14	15	
C15	20	
C16	25	
C17	30	
C18	35	

2.3. Characterization Methods

2.3.1. Mechanical Testing

A Kalpak (Nahre Gaon, Pune, India) KIC-2-1000 universal testing machine was used for tensile flexural testing with a digital load controller and elongation with a 100 kN load cell to test the tensile test at 28 °C and a humidity of $50 \pm 2\%$. In particular, for tensile testing, a 50 mm gauge length and a crosshead speed of 2 mm/min were applied. For flexural tests, a three-point fixture was used with 6 mm diameter pins with respective centers 75 mm apart from each other.

Izod impact testing was performed on a 15 J impactor by Deepak (Ahmedabad, Gujarat, India) with an impact speed equal to 3.46 m/s and an accuracy of 0.01 J. The mean value and standard deviation were reported for tests of five samples for each category. The specimens' dimensions and test standards are reported in Table 2.

Table 2. Standards and specimens' dimensions for mechanical testing.

Testing Mode	ASTM Standard	Specimens' Dimensions (mm)
Tensile	D3039	250 × 25 × 3
Flexural	D790	125 × 13 × 3
Izod impact	D256	65 × 13 × 3

2.3.2. Shore D Hardness Testing

The Shore-D hardness of the samples was measured using a Metrix Instruments (Kolkata, West Bengal 700001, India) durometer model RHTD, according to the ASTM D-2240 standard. For this purpose, specimens with dimensions of 20 × 20 × 3 mm were used. Each sample was measured ten times at different locations, and the average value obtained was taken. Following this, the mean value and standard deviation obtained from testing five samples in each category were reported.

The arrangement for sample removal for the different tests (tensile strength, flexural strength, Izod impact, and Shore D hardness) is depicted in Figure 2. One plate per variant was produced, considering the large number of them (nineteen) that were proposed. In each of them, the same disposition of samples was maintained.

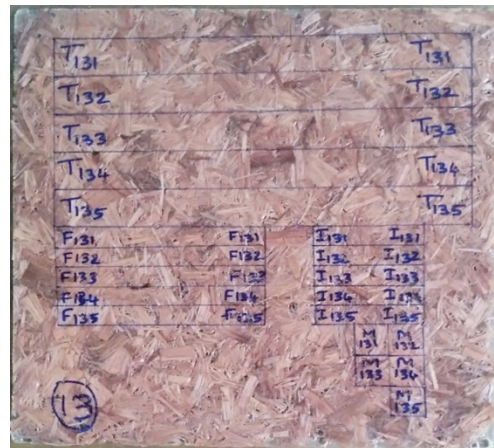


Figure 2. Composite plate prepared for the removal of four types of samples (tensile strength, flexural strength, Izod impact, Shore D hardness).

2.3.3. Thermal Characterization

Differential scanning calorimetry (DSC) was used to determine the glass transition temperature (T_g) and other transition events in composite samples. A DSC214 (NETZSCH GmbH & Co. Holding KG, Selb, Germany) apparatus was employed to record the heat exchange owing to thermal reactions that occurred during the heating and cooling of the composites. A temperature rate of 5 K/min was used for this scanning, and an acquisition rate of 300 points per minute was set up for this purpose.

Thermogravimetric analysis (TGA) was carried out using an apparatus model STA 449 F3 from NETZSCH GmbH & Co. Holding KG, Selb, Germany, to verify the thermal stability of the ACBF composite samples. The study was performed in a nitrogen gas (N_2) atmosphere at a heating rate of 10 °C/min with an acquisition rate of 300 points per minute in a temperature range of 50 to 700 °C.

3. Results and Discussion

The tensile data, namely the strength, modulus, and elongation to break, of the epoxy matrix and the randomly oriented short untreated *Acacia caesia* (ACB) bark fiber composites with varying fiber weight percentages and fiber lengths are reported in Figure 3.

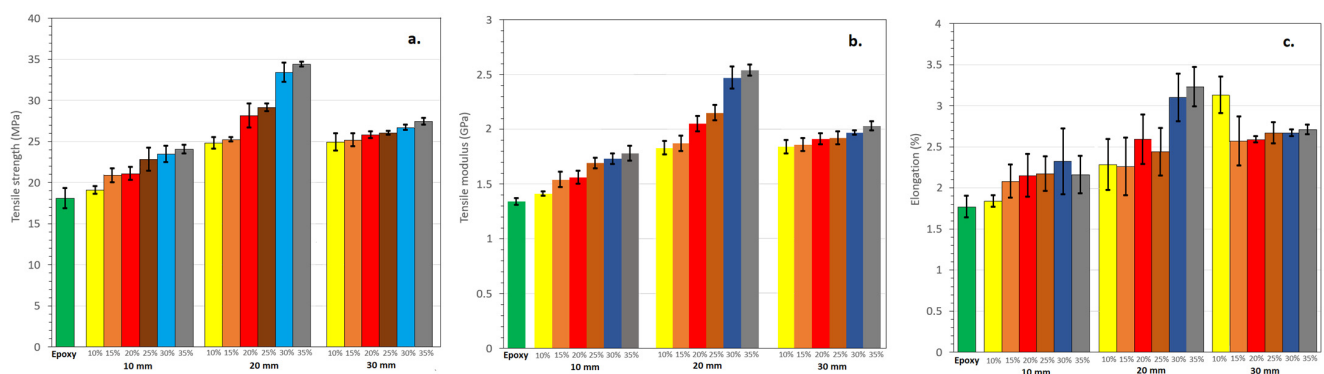


Figure 3. (a) Tensile strength; (b) tensile modulus; (c) elongation to break.

In particular, the tensile strength increased the higher the fiber content, up to the maximum fiber content of 35 wt.%. This can be attributed to more effective interfacial bonds between the fiber and the matrix, a promising outcome since this is normally offered in bark fibers only as a consequence of chemical treatment [32]. For all three tensile variables measured, i.e., strength, modulus, and strain to failure, the best configuration was that with 35 wt.% of 20-mm-long fibers, as clearly indicated in Figure 3. The effect of using

longer fibers was less defined; the maximum tensile strength of 34.41 MPa was obtained with 35% fibers 20 mm lengths, while composites with 30 mm fibers showed little benefit compared with 10 mm fibers. This was confirmed by the tensile modulus, which regularly increased with the fiber content, up to a value of 2.54 GPa for 35 wt.% of 20-mm-long fibers. Regarding fiber length, a significant increase in stiffness was observed with an increase in fiber length from 10 to 20 mm, which was not obtained with longer fibers of 30 mm. This was possibly due to the effect of defects in the fibers, which affected their deformation process during loading, leading to variable rigidity over their length [33]. Further considerations linked to elongation to break data suggest that the use of 20-mm-long fibers does allow the exploitation of a good part of the whole possible strain of the ACB fibers, which, according to data reported in [34], was in the region of 4.6 (± 1)% with 10% NaOH treatment. In this case, the maximum strain obtained was 3.23% (± 0.25) for 35 wt.% of 20-mm-long fibers. When introducing 30 mm fibers, the influence of defects became much more significant, as demonstrated by the large decrease in the strain at break with an increase from 10 wt.% to higher weight percentage. This might be attributed to the fact that fibers that are too long might contribute to insufficient fiber impregnation and, therefore, early failure triggered by the presence of defects.

It is suggested, therefore, that the introduction of this amount of untreated ACB fibers is possible and not detrimental to the composite. However, to find out which is the ideal fiber length, pullout studies would be required, such as suggested in [35]; these would require a further regularization of the diameter, which is likely not possible in untreated ACB fibers. It can also be suggested that the fibers reduce the strain variation between different samples, possibly smoothing the result of the presence of defects in the fibers. The maximal values obtained for tensile strength and stiffness compared favorably with most epoxy composites with short lignocellulosic fibers of comparable lengths and in similar amounts, as proven by the data reported in Table 3.

Table 3. Comparison of ACBF–epoxy composites with similar materials from literature.

Fiber	Weight (%)	Length (mm)	Tensile Strength (MPa)	Tensile Modulus (GPa)	Ref.
Banana	16%	15	16.12	0.64	[36]
Oil palm	5%	20	29.9	1.43	[37]
Kenaf	N. d.	40	31.3	3.75	[38]
<i>Lantana camara</i>	30%	100	19	1.17	[39]
<i>Eulaliopsis binata</i>	30%	11	21	-	[40]
<i>Acacia caesia</i>	35%	20	34.41	2.54	This study

In Figure 4, it is revealed that the flexural properties of ACB fiber epoxy composite were generally higher than those of pure epoxy, and their performance considerably grew with the fiber length. In particular, the composites including 25 wt.% of 30-mm-long fibers were those showing the maximum flexural strength and modulus, equal to 51.21 MPa and 2.83 GPa, respectively. This is attributed to the stronger bonding of the fiber and the matrix reported for that level of reinforcement fiber length. It is suggested, therefore, that under flexural loading, the non-uniformity of ACB fibers constitutes a lower limitation than that for tensile loading; therefore, the properties continue to increase up to a fiber length of 30 mm, which might be ascribed to a lower influence of defects on performance. Also, the fact that the flexural strength of ACB fiber composites grows steadily with the fiber weight is promising because even the highest amount of fiber introduced is practically applicable. Despite the difficulties in blending a higher fiber content, which is usual for irregular fibers and may lead to voids and ineffective defects in untreated fibers, treatment could promote an increase in the fiber–matrix bonding surface via the formation of interstices between fibrils [41].

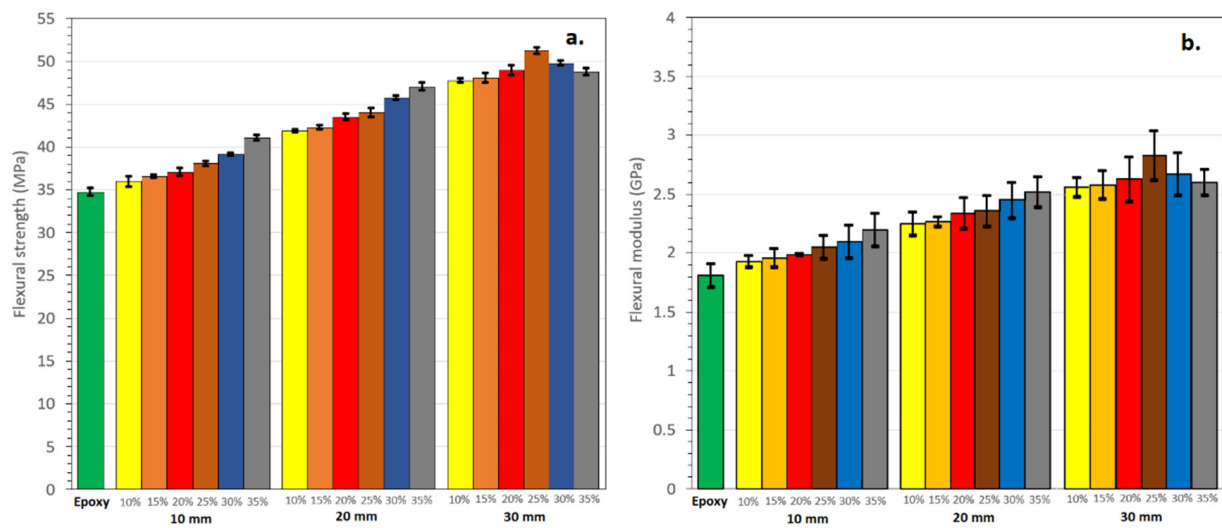


Figure 4. (a) Flexural strength; (b) flexural modulus of ACBF-epoxy composites.

A comparison of the flexural strength of various natural fiber-reinforced epoxy composites with untreated fibers is listed in Table 4 below. The performance offered by ACB fiber composites did effectively compare with the other fibers in the literature reported in the table; it is also important to note that ACB fibers compared quite favorably to the others, although they were much weaker than typical natural fibers for textile uses, such as sisal and kenaf.

Table 4. Comparison of the flexural strengths of ACBF-epoxy composites with those of other untreated short-fiber epoxy composites.

Fiber	Amount (wt. or vol. %)	Length (mm)	Flexural Strength (MPa)	Ref.
Outer banana bark	30 (wt.)	30	29.47	[42]
Middle banana bark	30 (wt.)	30	25.55	[42]
Inner banana bark	30 (wt.)	30	18.56	[42]
Midrib banana	30 (wt.)	30	22.57	[42]
Sisal	15 (wt.)	48	116.30	[43]
Pineapple leaf	15 (wt.)	1	48.63	[44]
Kenaf	38–41 (vol.)	80	235.13	[45]
Flax	40 (vol.)	15	66.07	[46]
<i>Acacia caesia</i> Bark	25 (wt.)	30	51.21	Present work

The effect of fiber loading on the impact strength of the *Acacia caesia* bark fiber composites is depicted in Figure 5a. The figure indicates that the impact strength increased with the introduction of more fibers in the composite, reaching the maximum value of 10.76 kJ/m² for composites with 35 wt.% of 20-mm-long fibers. At lower fiber loading levels, the impact strength was lower, possibly due to the presence of critical defects, such as voids and improper bonding at the interfacial regions, as is typical for limited concentrations of bark fibers in composites [47]. As the amount of reinforcement increased gradually, the supporting nature of cellulose present in the fiber was likely to neutralize the defects and transmit improved toughness [48]. Comparing the data obtained with those reported for the same content of other fibers in the epoxy matrix, as shown in Table 5, ACB fibers offered a comparable impact strength to the composites.

Concluding the section related to mechanical performance, it can be suggested that the presence of defects, such as dislocations, kinks, and microcompression [49], have a large influence on tensile properties, and increasing the length of the fibers might not result in an enhanced performance of the composite, which is instead observed in flexural loading. This is promising for the applicability of 30 mm-long fibers in *Acacia caesia* composites in the

sense that defects may create stress concentrations during flexure, whereas they typically open up during tension, such that, in general terms, the number of defects has an influence combined with that of fiber length [50]. This has been elsewhere to produce a decrease in flexural strength, e.g., on hemp fiber composites, but for a higher fiber length [51].

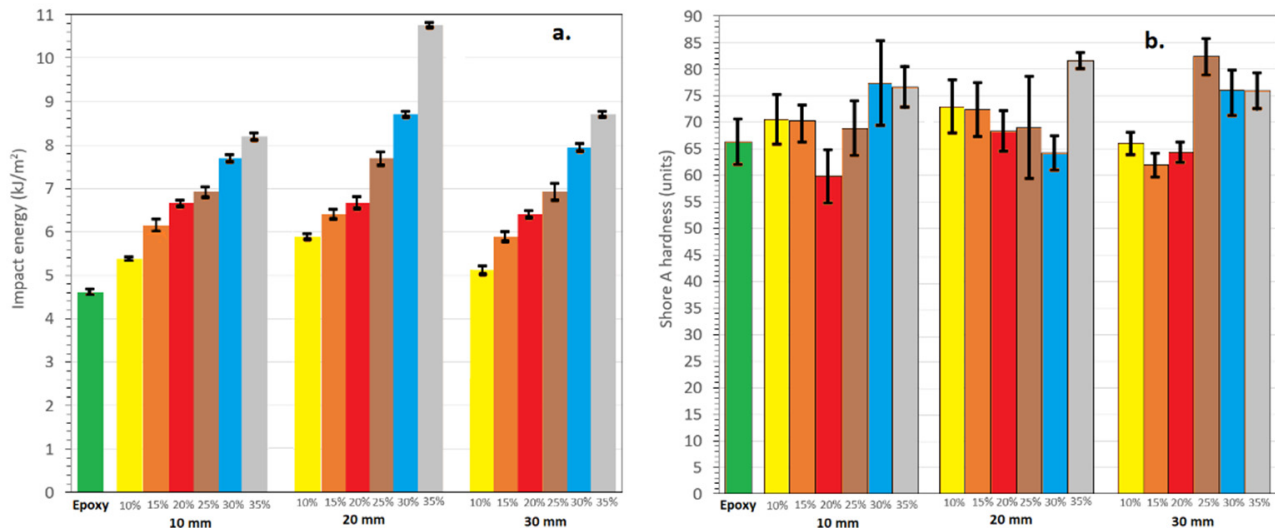


Figure 5. (a) Izod impact strength; (b) Shore D hardness of ACBF-epoxy composites.

Table 5. Comparison of impact strength with that of other epoxy composites with 35 wt.% untreated natural fibers.

Fiber	Impact Strength (kJ/m ²)	Ref.
Banana (undeclared length)	8.40	[52]
<i>Coccinia indica</i> (30 mm long)	7.38	[53]
<i>Lagenaria siceraria</i> (9 mm long)	11.31	[54]
<i>Acacia caesia</i> Bark (20 mm)	10.76	Present work

It can be also observed, as shown in Figure 5b, that increasing the wt.% and the length of the ACB fibers resulted in a noticeable effect on the hardness of the material. In comparison with pure epoxy, the hardness of all composites was observed to generally increase with the content of fibers introduced and their lengths, though with some exceptions. The presence of more abundant and longer ACB fibers in the composites, by enhancing the elasticity, also improved the surface resistance to indentation, yet it also induced some susceptibility to the state of the surface, roughened by the presence of more fibers. This was revealed to occur often with bark fibers [55], an issue that could be even worse in the case of alkali treatment [56].

As shown in Figures 6–8, the morphology of tensile fractured ACB-epoxy composites was investigated; the figures show the extreme fiber content cases: 10 and 35 wt.% composites with 10 mm-long (Figure 6), 20 mm-long (Figure 7), and 30 mm-long fibers (Figure 8). One sample from each category of ten images taken was selected, among which are those that are reported in this work.

In particular, in Figure 6a, it is possible to see that considerable voids were present due to trapped air, which is a possible occurrence when a limited amount of loosely packed filler is added [57]. Some fiber segments buckle into microfibrils during breakage. The failure seen is mostly due to failure of the matrix after fiber failure since more of the matrix phase is visible.

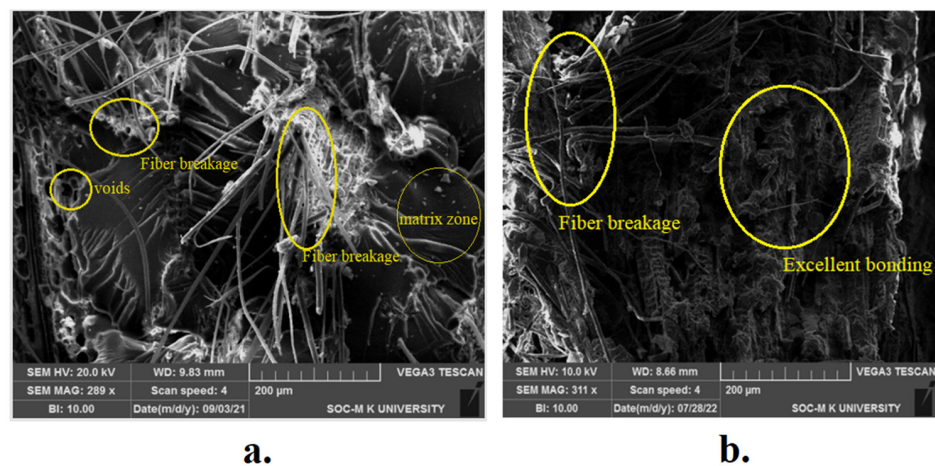


Figure 6. SEM micrographs of tensile-fractured samples with 10-mm-long ACB fibers: (a) 10 wt.% fibers (C1); (b) 35 wt.% fibers (C6).

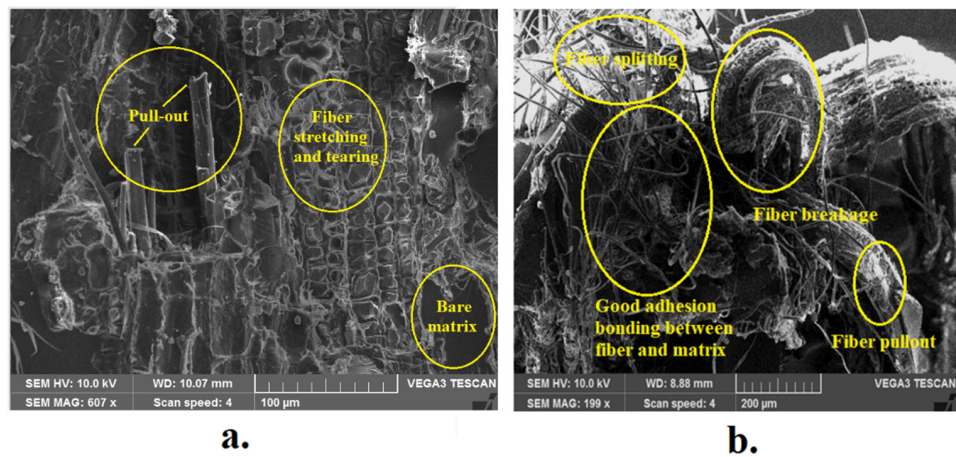


Figure 7. SEM micrographs of tensile-fractured samples with 20-mm-long ACB fibers: (a) 10 wt.% fibers (C7); (b) 35 wt.% fibers (C12).

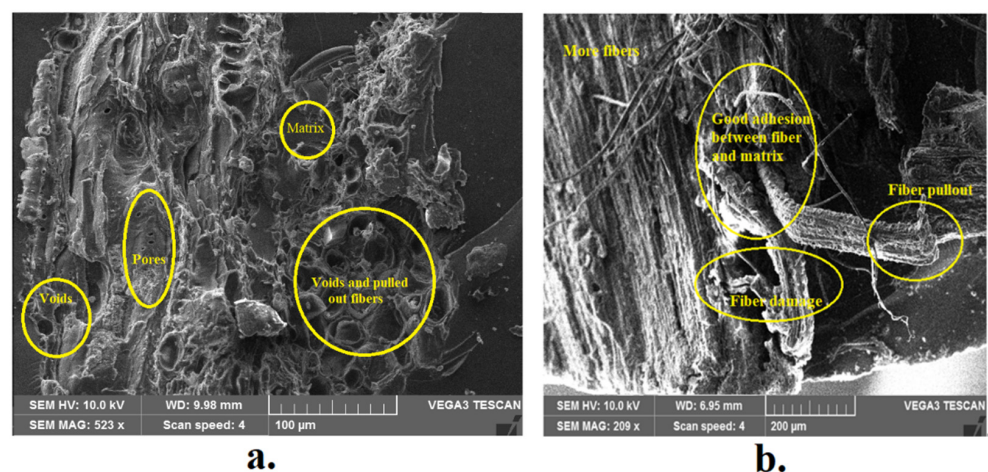


Figure 8. SEM micrographs of tensile-fractured samples with 30-mm-long ACB fibers: (a) 10 wt.% fibers (C13); (b) 35 wt.% fibers (C18).

The fiber length was increased to 20 mm (Figure 7); Figure 7a offers an indication of extensive fiber pullout from the matrix and fibers torn off during loading, which thus led to their fibrillation at the point of exiting the matrix. Again, non-negligible areas of the matrix without visible reinforcement were observed. Splitting and tearing are recognized as

frequent occurrences in natural fiber composites when the matrix behavior is prevalent [58]. By contrast, Figure 7b indicates a good strength of the fiber–matrix interface, while some areas still indicate fiber damage and splitting, which was suggested to occur in the absence of chemical treatment [34]. It is evident from the fibers depicted in the SEM image that the cell wall structure holds individual fibrils together to develop fiber networks, as reported in [59], and closely packed fiber distributions are possible despite the bark roughness.

Increasing the fiber length to the maximum value adopted, i.e., 30 mm (Figure 9), a larger contact area with the resin was obtained, at least in principle, even with only 10 wt.% fibers (Figure 9a). In practice, air penetration did not appear to be impeded, possibly because the longer fiber stretches introduced deviated from straightness, and therefore, their wettability by the matrix might not have been uniform [60]. However, as a whole, the improved interfacial adhesion between the fiber and the epoxy noticed in some fractured regions suggests an effective load transfer capability, which would explain the absence of decline observed in the flexural properties with respect to the composites with an equal content of shorter fibers.

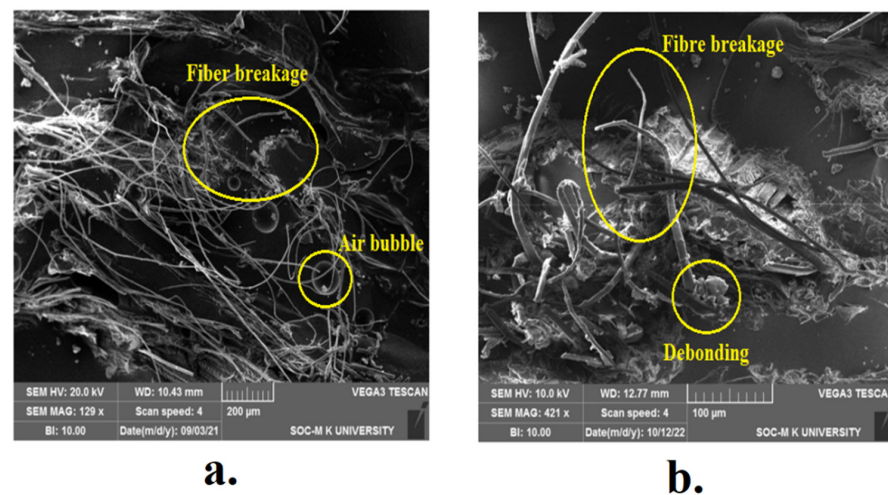


Figure 9. SEM micrographs of impact-fractured samples with 10-mm-long ACB fibers: (a) 20 wt.% fibers (C1); (b) 35 wt.% fibers (C6).

In Figures 9–11, the morphology of impact-fractured ACB–epoxy composites is reported, again showing the extreme fiber content cases: 10 and 35 wt.% composites with 10 mm (Figure 9), 20 mm (Figure 10), and 30 mm fibers (Figure 11).

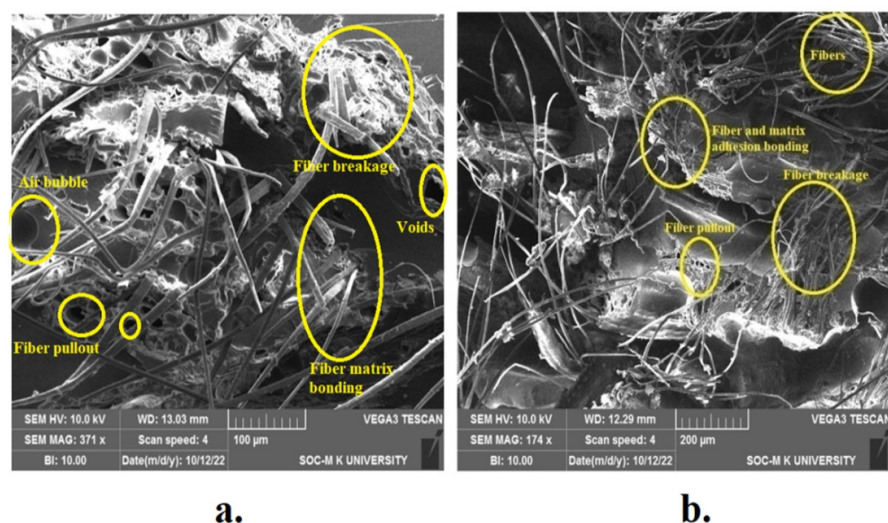


Figure 10. SEM micrographs of impact-fractured samples with 20-mm-long ACB fibers: (a) 10 wt.% fibers (C7); (b) 35 wt.% fibers (C12).

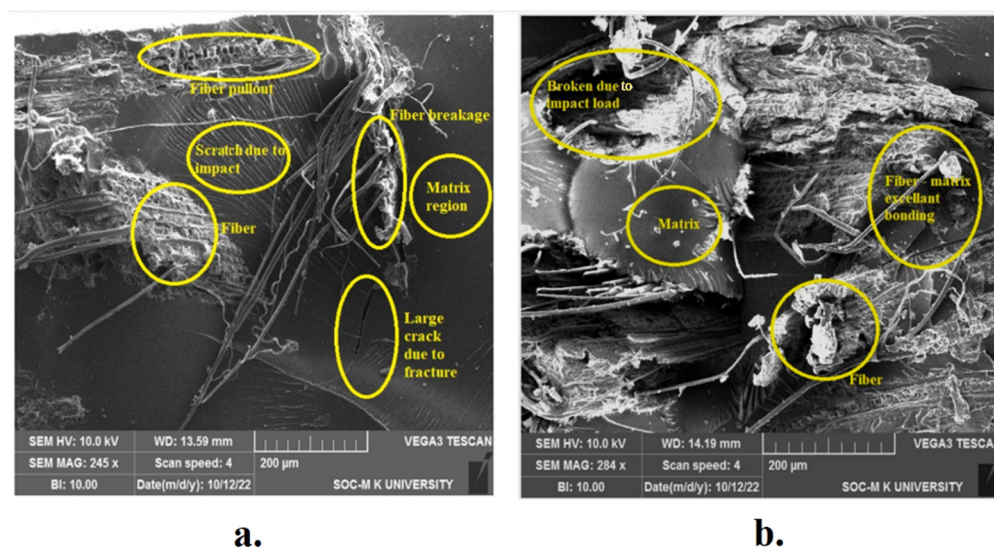


Figure 11. SEM micrographs of impact-fractured samples with 30-mm-long ACB fibers: (a) 20 wt.% fibers (C13); (b) 35 wt.% fibers (C18).

When using the shortest fiber set (10 mm), a large number of fractured fiber sites, one of which is especially highlighted, were observed in 10 wt.% impacted composite (Figure 9a), which suggests that the effect of reinforcement was very limited in this case. The presence of pullout and debonding phenomena was also abundant in 35 wt.% impacted composites (Figure 9b), though the fibers appeared more deformed than those in the previous case, which might indicate that they are more effective in the composite. When fiber length increased to 20 mm, it was noticed that the presence of pullouts was still very significant for 10 wt.% composites (Figure 10a), possibly due to the non-uniform distribution of fibers in the composite. By contrast, some areas of good bonding and composite collapse under impact with no evidence of pull-out were present in 35 wt.% composites (Figure 10b). This variability in pullout occurrence, due to geometrical mismatches of the fibers, is also typical of the most successfully used natural fibers, such as flax [61,62] and sisal [63], even after treatment. This may be considered to be of limited concern for untreated bark fibers, such as *Acacia caesia*, in which structural variations are particularly significant.

The thermogravimetric (TGA) curves for the composites with varying fiber lengths and wt.% are shown in Figure 12. In general terms, the composites with reinforcement showed slightly different thermal stabilities compared with those of the pure resin; however, the loss of weight due to non-structural material and hydration loss was very limited—no more than a few percent of the whole mass. The temperature interval in which the main degradation phenomena occur is approximately measured with a graphical method, as suggested in [64] and applied for untreated and treated ACB fibers in [26]. Four insets are taken from the curve, indicating (a) the initial release of moisture and decomposition of loosely connected materials, such as hemicellulose (a stage obviously absent in pure epoxy); (b) the onset of the main degradation stage; (c) the completion of the main degradation stage; and (d) the residue at 675 °C. In Table 6, the respective values of data elicited from the four insets in Figure 12 are reported. Some results are evident, particularly those regarding the degradation at a slightly lower temperature for the composites compared with the neat epoxy—specifically for the most effective one, i.e., the one with 35 wt.% of 20 mm-long fibers—although the differences between the various composite configurations are minimal. This also appears to be connected with the larger residue obtained at 675 °C for the composites compared with the neat epoxy. A comparison with the thermogravimetric results reported in [26] for untreated ACB fibers, which indicated degradation onset at 308 °C and a 20% residue remaining at 600 °C, shows that the present data are in line with the amounts of fiber introduced in the composites.

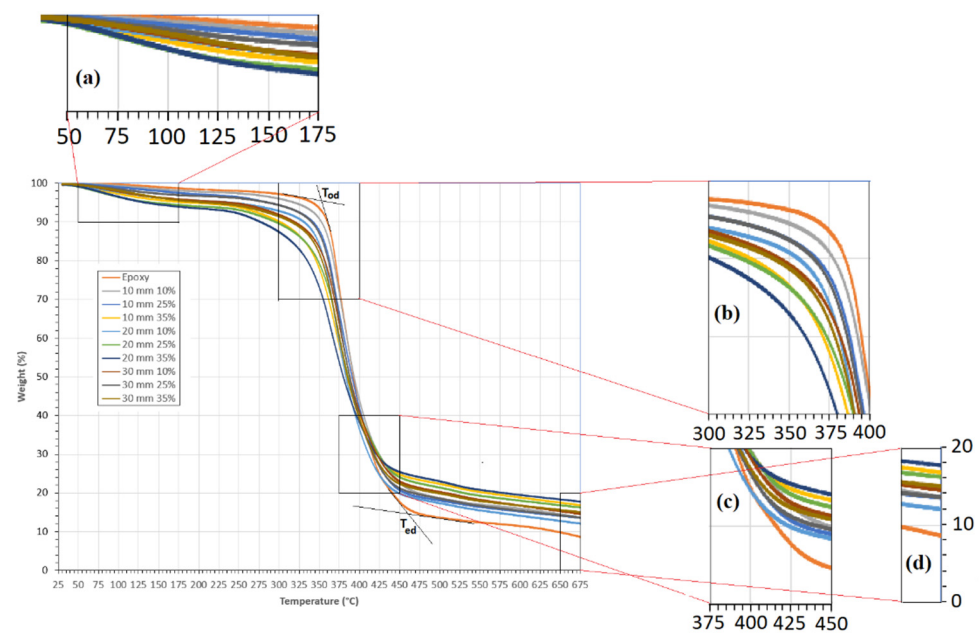


Figure 12. Thermogravimetric analysis (TGA) curves for ACBF-epoxy composites (T_{od} = onset degradation temperature; T_{ed} = end degradation temperature). The various insets represent: (a) 90–100% weight from 50 to 175 °C (decomposition of loose and non-structural matter); (b) 40–100% weight from 300 to 400 °C (onset of main degradation); (c) 20–40% weight from 375 to 450 °C (end of main degradation); (d) 0–20% weight from 650 to 675 °C (residue).

Table 6. Degradation characteristics (as from thermogravimetric studies).

Sample	Max. Moisture/Loose Materials Release (°C)	Onset Degradation (°C)	End Degradation (°C)	Residue at 675 °C (%)
Neat epoxy	-	367	456	9.3
10 mm 10 wt.%	104	362	408	13.7
10 mm 25 wt.%	110	360	411	13.5
10 mm 35 wt.%	123	340	417	16.8
20 mm 10 wt.%	108	340	418	12.2
20 mm 25 wt.%	121	352	415	16.2
20 mm 35 wt.%	125	333	409	17.8
30 mm 10 wt.%	113	346	416	14.5
30 mm 25 wt.%	116	359	414	14.8
30 mm 35 wt.%	121	345	412	14.7

From differential scanning calorimetry (DSC) curves reported in Figure 13, two insets are shown, which represent (a) moisture release and initial decomposition, as shown in the corresponding inset (a) of Figure 12; (b) the main degradation phenomena, as shown in the corresponding insets (b) and (c) of Figure 12. Compared with what was observed on other untreated bark fibers, it is supposed that some endothermic peaks showing the main degradation phenomena of cellulose are observable in the region between 300 and 350 °C; specifically, in [65], peaks were observed at 334.43 °C for *Grewia monticola* fibers. Other studies, such as studies on *Thespesia populnea* [66], have indicated a larger range for main degradation, namely between 250 and 375 °C, though starting with some initial phenomena around 175 °C, which appeared to be substantially suppressed and were not shown in these composites. As a general consideration, epoxy resin protects the fibers and allows them to withstand a temperature comparable to that of the matrix itself. On the other hand, it appears to be quite awkward to establish a trend between the degradation pattern of the

composites and the fiber content in terms of length and quantity since the endothermic peaks due to cellulose degradation never appear below 320 °C but have variable intensity at unpredictable temperatures. It is suggested that the changing strength of fiber–matrix interface results in an equally scattered thermal behavior of the composite.

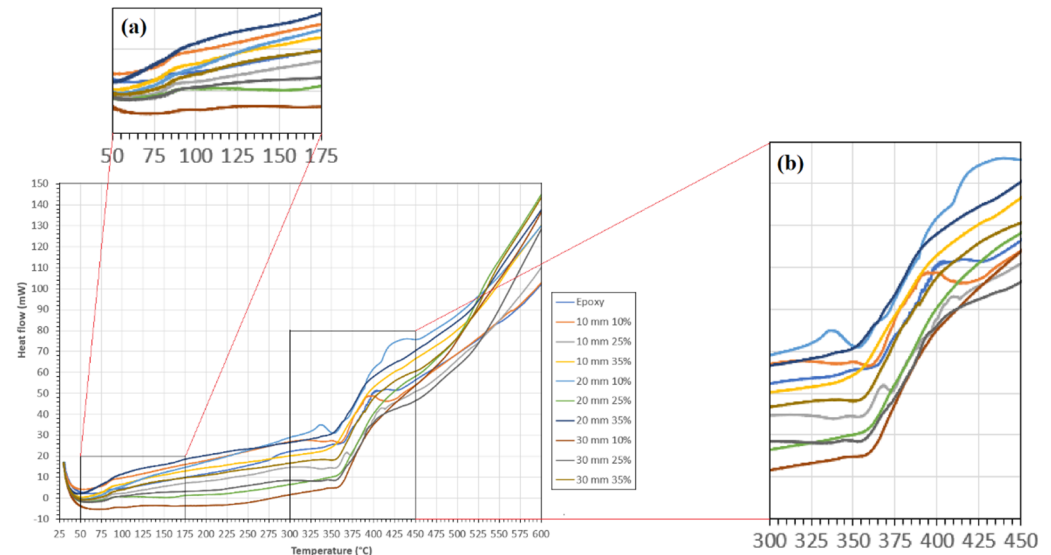


Figure 13. Differential scanning calorimetry (DSC) curves for ACBF-epoxy composites. Insets: (a) Moisture/Non-structural material release (50–175 °C); (b) Principal degradation phenomena (300–450 °C).

4. Conclusions

The objective of this study was to produce epoxy composites using newly identified bark fibers extracted from *Acacia caesia* without treating them chemically with the understanding from previous investigations that a substantial amount of chemicals would have to be applied to make them sufficiently regular. The results indicated that the interface strength was adapted, at least for a fiber length not exceeding 20 mm, to offer improved properties to the composite in terms of tensile strength, flexural strength, Izod impact, and Shore D hardness. Due to the variable geometry of the fibers, air penetration was never completely impeded by the compression molding process adopted, and therefore, fiber–matrix bonding was not always optimal, which suggests possible chances for improvement. However, the thermal properties were not far from those of the resin alone, which indicates that *Acacia caesia* may represent an adapted reinforcement for epoxy, as an alternative to other bark fibers that have received growing attention over the past years as by-products or waste of other production systems.

Author Contributions: Conceptualization, S.P. and R.N.; methodology, S.P. and M.P.; validation, M.K. and C.S.; formal analysis, M.P. and C.F.; investigation, S.P., R.N. and M.K.; resources, C.S.; data curation, C.F.; writing—original draft preparation, S.P., M.K. and M.P.; writing—review and editing, C.S. and C.F.; visualization, C.S.; supervision, M.K.; project administration, M.K.; funding acquisition, C.S. All authors have read and agreed to the published version of the manuscript.

Funding: This research received no external funding.

Data Availability Statement: Data are available upon request.

Conflicts of Interest: The authors declare no conflict of interest.

References

- Bouras, M.; Chadni, M.; Barba, F.J.; Grimi, N.; Bals, O.; Vorobiev, E. Optimization of microwave-assisted extraction of polyphenols from *Quercus* bark. *Ind. Crops Prod.* **2015**, *77*, 590–601. [\[CrossRef\]](#)
- Nahrstedt, A.; Schmidt, M.; Jäggi, R.; Metz, J.; Khayyal, M.T. Willow bark extract: The contribution of polyphenols to the overall effect. *Wien. Med. Wochenschr.* **2007**, *157*, 348–351. [\[CrossRef\]](#)
- Ghitescu, R.-E.; Volf, I.; Carausu, C.; Bühlmann, A.-M.; Gilca, I.A.; Popa, V.I. Optimization of ultrasound-assisted extraction of polyphenols from spruce wood bark. *Ultrason. Sonochem.* **2015**, *22*, 535–541. [\[CrossRef\]](#)
- Banso, A. Phytochemical and antibacterial investigation of bark extracts of *Acacia nilotica*. *J. Med. Plant Res.* **2009**, *3*, 082–085.
- Maimoona, A.; Naeem, I.; Saddiqe, Z.; Jameel, K. A review on biological, nutraceutical and clinical aspects of French maritime pine bark extract. *J. Ethnopharmacol.* **2011**, *133*, 261–277. [\[CrossRef\]](#) [\[PubMed\]](#)
- Lee, Y.S.; Ryu, M.J. Antioxidant Effects of Cinnamomum cassia Bark Extract and its Effectiveness as a Cosmetics Ingredient. *Asian J. Beauty Cosmetol.* **2019**, *17*, 69–80. [\[CrossRef\]](#)
- Haghibin, M.R.; Shahrak, M.N. Process conditions optimization for the fabrication of highly porous activated carbon from date palm bark wastes for removing pollutants from water. *Powder Technol.* **2021**, *377*, 890–899. [\[CrossRef\]](#)
- Yadav, N.; Ritu, Promila; Hashmi, S. A Hierarchical porous carbon derived from eucalyptus-bark as a sustainable electrode for high-performance solid-state supercapacitors. *Sustain. Energy Fuels* **2020**, *4*, 1730–1746. [\[CrossRef\]](#)
- Sienkiewicz, N.; Dominic, M.; Parameswaranpillai, J. Natural Fillers as Potential Modifying Agents for Epoxy Composition: A Review. *Polymers* **2022**, *14*, 265. [\[CrossRef\]](#) [\[PubMed\]](#)
- Vinod, A.; Gowda, T.Y.; Vijay, R.; Sanjay, M.; Gupta, M.K.; Jamil, M.; Kushvaha, V.; Siengchin, S. Novel *Muntingia calabura* bark fiber reinforced green-epoxy composite: A sustainable and green material for cleaner production. *J. Clean. Prod.* **2021**, *294*, 126337. [\[CrossRef\]](#)
- Balasubramanian, B.; Raja, K.; Kumar, V.V.; Ganeshan, P. Characterization study of *Holoptelea integrifolia* tree bark fibres reinforced epoxy composites. *Nat. Prod. Res.* **2022**, 1–10, published online 1 November 2022. [\[CrossRef\]](#)
- Reddy, P.V.; Mohana Krishnudu, D.; Rajendra Prasad, P. A study on alkali treatment influence on *Prosopis juliflora* fiber-reinforced epoxy composites. *J. Nat. Fib.* **2021**, *18*, 1094–1106. [\[CrossRef\]](#)
- Rajan, B.S.; Saibalaji, M.A.; Mohideen, S.R. Tribological performance evaluation of epoxy modified phenolic FC reinforced with chemically modified *Prosopis juliflora* bark fiber. *Mater. Res. Express* **2019**, *6*, 075313. [\[CrossRef\]](#)
- Gurupranes, S.V.; Rajendran, I.; Shanmuga Sundaram, N. Suitability assessment of raw-alkalized *Ziziphus nummularia* bark fibers and its polymeric composites for lightweight applications. *Polym. Compos.* **2022**, *43*, 5059–5075. [\[CrossRef\]](#)
- Bogoeva-Gaceva, G.; Avella, M.; Malinconico, M.; Buzarovska, A.; Grozdanov, A.; Gentile, G.; Errico, M.E. Natural fiber eco-composites. *Polym. Compos.* **2007**, *28*, 98–107. [\[CrossRef\]](#)
- De Paola, S.; Fragassa, C.; Minak, G.; Pavlovic, A. Green composites: A review of state of art. In Proceedings of the 30th Danubia-Adria Symposium on Advances in Experimental Mechanics, (DAS 2013), 77–78, Code 125164, Primošten, Croatia, 25–28 September 2013.
- Santulli, C.; Fragassa, C.; Pavlovic, A.; Nikolic, D. Use of Sea Waste in Composite Materials: A Review. *J. Mar. Sci. Eng.* **2023**, *11*, 855. [\[CrossRef\]](#)
- Bertomeu, D.; García-Sanoguera, D.; Fenollar, O.; Boronat, T.; Balart, R. Use of eco-friendly epoxy resins from renewable resources as potential substitutes of petrochemical epoxy resins for ambient cured composites with flax reinforcements. *Polym. Compos.* **2012**, *33*, 683–692. [\[CrossRef\]](#)
- Fragassa, C.; de Camargo, F.V.; Pavlovic, A.; Minak, G. Experimental evaluation of static and dynamic properties of low styrene emission vinylester laminates reinforced by natural fibres. *Polym. Test.* **2018**, *69*, 437–449. [\[CrossRef\]](#)
- Alves Fidelis, M.E.; Pereira, T.V.C.; Gomes, O.d.F.M.; de Andrade Silva, F.; Toledo Filho, R.D. The effect of fiber morphology on the tensile strength of natural fibers. *J. Mater. Res. Technol.* **2013**, *2*, 149–157. [\[CrossRef\]](#)
- George, J.; Sreekala, M.S.; Thomas, S. A review on interface modification and characterization of natural fiber reinforced plastic composites. *Polym. Eng. Sci.* **2001**, *41*, 1471–1485. [\[CrossRef\]](#)
- Sundaram, R.S.; Rajamoni, R.; Suyambulingam, I.; Isaac, R. Comprehensive Characterization of Industrially Discarded *Cymbopogon flexuosus* Stem Fiber Reinforced Unsaturated Polyester Composites: Effect of Fiber Length and Weight Fraction. *J. Nat. Fibers* **2022**, *19*, 7241–7256. [\[CrossRef\]](#)
- Venkata Smitha, P.; Ch, M.M.; Kandra, P.; Sravani, R.; Akondi, R.B. Screening of antimicrobial and antioxidant potentials of *Acacia caesia*, *Dillenia pentagyna* and *Buchanania lanzan* from Maredumilli forest of India. *J. Pharm. Res.* **2012**, *5*, 1734–1738.
- Ashwini, J.; Aswathy, T.R.; Rahul, A.B.; Thara, G.M.; Nair, A.S. Synthesis and Characterization of Zinc Oxide Nanoparticles Using *Acacia caesia* Bark Extract and Its Photocatalytic and Antimicrobial Activities. *Catalysts* **2021**, *11*, 1507. [\[CrossRef\]](#)
- Thomas, S.K.; Begum, P.M.S.; Dominic, C.D.M.; Salim, N.V.; Hameed, N.; Rangappa, S.M.; Siengchin, S.; Parameswaranpillai, J. Isolation and characterization of cellulose nanowhiskers from *Acacia caesia* plant. *J. Appl. Polym. Sci.* **2020**, *138*, 50213. [\[CrossRef\]](#)
- Sivasubramanian, P.; Kalimuthu, M.; Palaniappan, M.; Alavudeen, A.; Rajini, N.; Santulli, C. Effect of Alkali Treatment on the Properties of *Acacia caesia* Bark Fibres. *Fibers* **2021**, *9*, 49. [\[CrossRef\]](#)
- Palanisamy, S.; Mayandi, K.; Dharmalingam, S.; Rajini, N.; Santulli, C.; Mohammad, F.; Al-Lohedan, H.A. Tensile Properties and Fracture Morphology of *Acacia caesia* Bark Fibers Treated with Different Alkali Concentrations. *J. Nat. Fibers* **2022**, *19*, 11258–11269. [\[CrossRef\]](#)

28. John, M.J.; Varughese, K.T.; Thomas, S. Green Composites from Natural Fibers and Natural Rubber: Effect of Fiber Ratio on Mechanical and Swelling Characteristics. *J. Nat. Fibers* **2008**, *5*, 47–60. [\[CrossRef\]](#)
29. Venkateshwaran, N.; ElayaPerumal, A.; Jagatheeshwaran, M.S. Effect of fiber length and fiber content on mechanical properties of banana fiber/epoxy composite. *J. Reinf. Plast. Compos.* **2011**, *30*, 1621–1627. [\[CrossRef\]](#)
30. Ghali, L.; Msahli, S.; Zidi, M.; Sakli, F. Effects of Fiber Weight Ratio, Structure and Fiber Modification onto Flexural Properties of Luffa-Polyester Composites. *Adv. Mater. Phys. Chem.* **2011**, *1*, 78–85. [\[CrossRef\]](#)
31. Migneault, S.; Koubaa, A.; Erchiqui, F.; Chaala, A.; Englund, K.; Krause, C.; Wolcott, M. Effect of fiber length on processing and properties of extruded wood-fiber/HDPE composites. *J. Appl. Polym. Sci.* **2008**, *110*, 1085–1092. [\[CrossRef\]](#)
32. Nurazzi, N.M.; Khalina, A.; Sapuan, S.M.; Ilyas, R.A. Mechanical properties of sugar palm yarn/woven glass fiber reinforced unsaturated polyester composites: Effect of fiber loadings and alkaline treatment. *Polymers* **2019**, *64*, 665–675. [\[CrossRef\]](#)
33. Kumar, S.S.; Raja, V.M. Processing and determination of mechanical properties of *Prosopis juliflora* bark, banana and coconut fiber reinforced hybrid bio composites for an engineering field. *Compos. Sci. Technol.* **2021**, *208*, 108695. [\[CrossRef\]](#)
34. Hughes, M. Defects in natural fibres: Their origin, characteristics and implications for natural fibre-reinforced composites. *J. Mater. Sci.* **2011**, *47*, 599–609. [\[CrossRef\]](#)
35. Liu, Y.; Ma, Y.; Yu, J.; Zhuang, J.; Wu, S.; Tong, J. Development and characterization of alkali treated abaca fiber reinforced friction composites. *Compos. Interfaces* **2018**, *26*, 67–82. [\[CrossRef\]](#)
36. Venkateshwaran, N.; ElayaPerumal, A.; Alavudeen, A.; Thiruchitrambalam, M. Mechanical and water absorption behaviour of banana/sisal reinforced hybrid composites. *Mater. Des.* **2011**, *32*, 4017–4021. [\[CrossRef\]](#)
37. Yusoff, M.Z.M.; Salit, M.S.; Ismail, N.; Wirawan, R. Mechanical properties of short random oil palm fibre reinforced epoxy composites. *Sains Malays.* **2010**, *39*, 87–92.
38. Fiore, V.; Di Bella, G.; Valenza, A. The effect of alkaline treatment on mechanical properties of kenaf fibers and their epoxy composites. *Compos. Part B: Eng.* **2015**, *68*, 14–21. [\[CrossRef\]](#)
39. Bhupender, A.K. Study on mechanical behaviour of lantana-camara fiber reinforced epoxy-based composites. *Int. Res. J. Eng. Technol.* **2017**, *4*, 3167–3171.
40. Pradhan, S.; Acharya, S.K.; Prakash, V. Mechanical, morphological, and tribological behavior of Eulaliopsis binata fiber epoxy composites. *J. Appl. Polym. Sci.* **2021**, *138*, 50077. [\[CrossRef\]](#)
41. Shariff, M.D.; Madhu, S.; Palani, K.. Suitability Evaluation of Mercerized Albizia Julibrissin Fiber as a Potential Reinforcement for Bio-composites. *J. Nat. Fibers* **2021**, *19*, 8383–8398. [\[CrossRef\]](#)
42. Motaleb, K.Z.M.A.; Ahad, A.; Laureckiene, G.; Milasius, R. Innovative Banana Fiber Nonwoven Reinforced Polymer Composites: Pre- and Post-Treatment Effects on Physical and Mechanical Properties. *Polymers* **2021**, *13*, 3744. [\[CrossRef\]](#) [\[PubMed\]](#)
43. Webo, W.; Maringa, M.; Masu, L. The tensile and flexural properties of treated and untreated sisal fibre-epoxy resin composites. *Int. J. Mech Mechatron Eng.* **2019**, *19*, 27–40.
44. Yousif, B.F.; Shalwan, A.; Chin, C.W.; Ming, K.C. Flexural properties of treated and untreated kenaf/epoxy composites. *Mater Des.* **2012**, *40*, 378–385. [\[CrossRef\]](#)
45. Suarsana, I.; Suryawan, I.; Suardana, N.; Winaya, S.; Soenoko, R.; Suyasa, B.; Sunu, W.; Rasta, M. Flexural strength of hybrid composite resin epoxy reinforced stinging nettle fiber with silane chemical treatment. *AIMS Mater. Sci.* **2021**, *8*, 185–199. [\[CrossRef\]](#)
46. Amroune, S.; Belaadi, A.; Dalmis, R.; Seki, Y.; Makhoul, A.; Satha, H. Quantitatively Investigating the effects of fiber parameters on tensile and flexural response of flax/epoxy biocomposites. *J. Nat. Fibers* **2022**, *19*, 2366–2381. [\[CrossRef\]](#)
47. Vinod, A.; Sanjay, M.R.; Siengchin, S. Fatigue and thermo-mechanical properties of chemically treated Morinda citrifolia fiber-reinforced bio-epoxy composite: A sustainable green material for cleaner production. *J. Clean. Prod.* **2021**, *326*, 129411. [\[CrossRef\]](#)
48. Karnani, R.; Krishnan, M.; Narayan, R. Biofiber-reinforced polypropylene composites. *Polym. Eng. Sci.* **1997**, *37*, 476–483. [\[CrossRef\]](#)
49. Le Guen, M.J.; Newman, R.H. Pulped Phormium tenax leaf fibres as reinforcement for epoxy composites. *Compos. Part A Appl. Sci. Manuf.* **2007**, *38*, 2109–2115. [\[CrossRef\]](#)
50. Baley, C. Influence of kink bands on the tensile strength of flax fibers. *J. Mater. Sci.* **2004**, *39*, 331–334. [\[CrossRef\]](#)
51. Sawpan, M.A.; Pickering, K.L.; Fernyhough, A. Flexural properties of hemp fibre reinforced polylactide and unsaturated polyester composites. *Compos. Part A Appl. Sci. Manuf.* **2011**, *43*, 519–526. [\[CrossRef\]](#)
52. Jayaseelan, C.; Padmanabhan, P.; Athijayamani, A.; Ramanathan, K. Comparative Investigation of Mechanical Properties of Epoxy Composites Reinforced with Short Fibers, Macro Particles, and Micro Particles. *Bioresources* **2017**, *12*, 2864–2871. [\[CrossRef\]](#)
53. Bhuvaneshwaran, M.; Sampath, P.; Sagadevan, S. Influence of fiber length, fiber content and alkali treatment on mechanical properties of natural fiber-reinforced epoxy composites. *Polimery* **2019**, *64*, 93–99. [\[CrossRef\]](#)
54. Nagappan, S.; Subramani, S.P.; Palaniappan, S.K.; Mysamy, B. Impact of alkali treatment and fiber length on mechanical properties of new agro waste *Lagenaria Siceraria* fiber reinforced epoxy composites. *J. Nat. Fibers* **2021**, *19*, 6853–6864. [\[CrossRef\]](#)
55. Palanisamy, S.; Kalimuthu, M.; Nagarajan, R.; Marlet, J.M.F.; Santulli, C. Physical, Chemical, and Mechanical Characterization of Natural Bark Fibers (NBFs) Reinforced Polymer Composites: A Bibliographic Review. *Fibers* **2023**, *11*, 13. [\[CrossRef\]](#)

56. Narayanasamy, P.; Balasundar, P.; Senthil, S.; Sanjay, M.R.; Siengchin, S.; Khan, A.; Asiri, A.M. Characterization of a novel natural cellulosic fiber from *Calotropis gigantea* fruit bunch for ecofriendly polymer composites. *Int. J. Biol. Macromol.* **2020**, *150*, 793–801. [[CrossRef](#)] [[PubMed](#)]
57. Vivek, S.; Kanthavel, K. Effect of bagasse ash filled epoxy composites reinforced with hybrid plant fibres for mechanical and thermal properties. *Compos. Part B: Eng.* **2018**, *160*, 170–176. [[CrossRef](#)]
58. Herrera-Franco, P.; Valadez-Gonzalez, A. A study of the mechanical properties of short natural-fiber reinforced composites. *Compos. Part B Eng.* **2005**, *36*, 597–608. [[CrossRef](#)]
59. Kathirselvam, M.; Kumaravel, A.; Arthanarieswaran, V.; Saravanakumar, S. Assessment of cellulose in bark fibers of *Thespesia populnea*: Influence of stem maturity on fiber characterization. *Carbohydr. Polym.* **2019**, *212*, 439–449. [[CrossRef](#)]
60. De Rosa, I.M.; Kenny, J.M.; Puglia, D.; Santulli, C.; Sarasini, F. Morphological, thermal and mechanical characterization of okra (*Abelmoschus esculentus*) fibres as potential reinforcement in polymer composites. *Compos. Sci. Technol.* **2010**, *70*, 116–122. [[CrossRef](#)]
61. Baley, C.; Gomina, M.; Breard, J.; Bourmaud, A.; Davies, P. Variability of mechanical properties of flax fibres for composite reinforcement. A review. *Ind. Crops Prod.* **2019**, *145*, 111984. [[CrossRef](#)]
62. Georgiopoulos, P.; Christopoulos, A.; Koutsoumpis, S.; Kontou, E. The effect of surface treatment on the performance of flax/biodegradable composites. *Compos. Part B Eng.* **2016**, *106*, 88–98. [[CrossRef](#)]
63. Fiore, V.; Scalici, T.; Nicoletti, F.; Vitale, G.; Prestipino, M.; Valenza, A. A new eco-friendly chemical treatment of natural fibres: Effect of sodium bicarbonate on properties of sisal fibre and its epoxy composites. *Compos. Part B Eng.* **2015**, *85*, 150–160. [[CrossRef](#)]
64. Liu, Z.Q.; Yi, X.-S.; Feng, Y. Effects of glycerin and glycerol monostearate on performance of thermoplastic starch. *J. Mater. Sci.* **2001**, *36*, 1809–1815. [[CrossRef](#)]
65. Almeshaal, M.; Palanisamy, S.; Murugesan, T.M.; Palaniappan, M.; Santulli, C. Physico-chemical characterization of *Grewia Monticola* Sond (GMS) fibers for prospective application in biocomposites. *J. Nat. Fibers* **2022**, *19*, 15276–15290. [[CrossRef](#)]
66. Kathirselvam, M.; Kumaravel, A.; Arthanarieswaran, V.P.; Saravanakumar, S.S. Isolation and characterization of cellulose fibers from *Thespesia populnea* barks: A study on physicochemical and structural properties. *Int. J. Biol. Macromol.* **2019**, *129*, 396–406. [[CrossRef](#)] [[PubMed](#)]

Disclaimer/Publisher's Note: The statements, opinions and data contained in all publications are solely those of the individual author(s) and contributor(s) and not of MDPI and/or the editor(s). MDPI and/or the editor(s) disclaim responsibility for any injury to people or property resulting from any ideas, methods, instructions or products referred to in the content.